

1 Complete decoupling of bacterial growth from biopolymer production
2 through proteolytic control of enzyme levels

3
4 by

5
6 Gonzalo Durante-Rodríguez¹, Víctor de Lorenzo^{2*}, and Pablo I. Nikel^{3*}

7
8 ¹ Environmental Microbiology Group, Centro de Investigaciones Biológicas (CIB-CSIC), 28040
9 Madrid, Spain

10 ² Systems and Synthetic Biology Program, Centro Nacional de Biotecnología (CNB-CSIC),
11 28049 Madrid, Spain

12 ³ Systems Environmental Microbiology Group, The Novo Nordisk Foundation Center for
13 Biosustainability, Technical University of Denmark, 2800 Kgs Lyngby, Denmark

14
15 Running headline: Proteolysis-based control of metabolism

16 Keywords: Synthetic biology · Metabolic engineering · Proteolysis · *Escherichia coli*
17 · PHB · Pathway engineering

18
19
20 * Correspondence to: *Pablo I. Nikel* (pabnik@biosustain.dtu.dk)

21 The Novo Nordisk Foundation Center for Biosustainability,

22 Technical University of Denmark

23 2800 Lyngby, Denmark

24 Tel: (+45 93) 51 19 18

25 *Víctor de Lorenzo* (vdlorenzo@cnb.csic.es)

26 Centro Nacional de Biotecnología (CNB-CSIC)

27 28049 Madrid, Spain

28 Tel: (+34 91) 585 45 73

29
30

1 ABSTRACT

2

3 Most current methods for controlling the rate of formation of a key protein or enzyme in cell
4 factories rely on the manipulation of target genes within the pathway. In this article, we present a
5 novel synthetic system for post-translational regulation of protein levels, *FENIX*, which provides
6 both independent control of the steady-state protein level and inducible accumulation of targeted
7 proteins. The device is based on the constitutive, proteasome-dependent degradation of the
8 target polypeptide by tagging with a short synthetic, hybrid Nla/SsrA amino acid sequence in the
9 C-terminal domain. The protein degradation process can be reversed by activating the system *via*
10 addition of an orthogonal inducer (e.g. 3-methylbenzoate) to the culture medium. The system was
11 benchmarked in *Escherichia coli* by tagging two fluorescent proteins (GFP and mCherry) and
12 further exploited for engineering poly(3-hydroxybutyrate) (PHB) accumulation completely
13 uncoupled from bacterial growth. By tagging PhaA (3-ketoacyl-CoA thiolase, first step of the
14 route), a dynamic metabolic switch at the acetyl-coenzyme A node was established in such a way
15 that this metabolic precursor could be effectively directed into PHB formation upon activation of
16 the system. The engineered *E. coli* strain reached a very high specific rate of PHB accumulation
17 with a polymer content of ca. 72% (w/w) in glucose cultures set in the growth-decoupled mode.
18 Thus, *FENIX* enables dynamic control of metabolic fluxes in bacterial cell factories by establishing
19 post-translational synthetic switches in the pathway of interest.

20

21 GRAPHICAL ABSTRACT

22

23

24

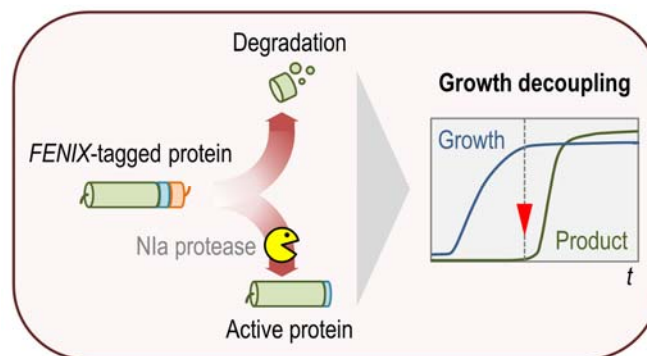
25

26

27

28

29



1 INTRODUCTION

2

3 One of the main challenges in contemporary metabolic engineering is to develop systems for
4 controlling enzyme activities in a spatial-temporal fashion, leading to the highest possible catalytic
5 output¹⁻². The problem can be tackled by manipulating genes and proteins at different levels of
6 regulation in cell factories. Transcriptional and translational regulation mechanisms, for instance,
7 have been studied in great detail in many biotechnologically-relevant microorganisms, and
8 several studies describe synthetic circuits exploiting these cellular processes for practical
9 purposes³⁻⁶. More recently, the adoption of CRISPR/Cas9-mediated technologies has opened up
10 countless possibilities for targeted regulation at the gene/genome level⁷⁻⁸. The conditional and
11 dynamic control of protein levels *in vivo*, in contrast, has received less attention thus far, and the
12 majority of the currently available tools designed to modulate protein activity target mRNAs and
13 protein synthesis rates (e.g. by using specific transcriptional repressors, RNA interference
14 strategies, and riboregulators). Some synthetic devices for the tunable control of protein synthesis
15 and degradation have been developed over the last few years⁹, e.g. systems triggered by small
16 molecules¹⁰⁻¹² or indirect degradation processes¹³⁻¹⁵. From a practical perspective, these
17 strategies allow for a tight and accurate control of metabolic pathways since the transcriptional or
18 translational regulation of the gene(s) encoding the target(s) are not altered.

19

20 Yet, as good as devices for controlling heterologous expression may be, most approaches for
21 bioproduction of added-value compounds rely on growth-coupled biosynthesis, because
22 constitutive expression of the genes in the target pathway is easier and simpler than inducing
23 product accumulation after microbial growth. However, growth-coupled production severely limits
24 product yield and productivity¹⁶⁻¹⁷. Biomass formation can consume up to 60% of the carbon
25 source across different cultivation techniques. This situation is particularly relevant for products
26 synthesized from precursors of central carbon metabolism that also serve as building-blocks for
27 biomass formation. Bacterial polyhydroxyalkanoates (PHAs), biodegradable polyesters with a
28 broad range of interesting biotechnological applications¹⁸⁻¹⁹, constitute such an example, as they
29 are synthesized from acetyl-coenzyme A (CoA) as the main precursor²⁰. PHA production in
30 recombinant *Escherichia coli* strains has mostly exploited growth-associated polymer
31 accumulation²¹⁻²², which creates a competition for acetyl-CoA between biomass formation and

1 PHA synthesis²³—potentially leading to metabolic imbalances that hinder high levels of product
2 accumulation. In this context, the question at stake is whether growth and production phases
3 could be uncoupled by repurposing natural molecular mechanisms known to control protein
4 integrity and functionality once the cognate mRNAs have been translated.

5

6 Protein degradation in bacteria is mediated by several processes²⁴. One of them is the so called
7 *transfer-messenger RNA* (tmRNA) system, based on special RNA molecules that function both as
8 tRNAs and mRNAs. tmRNAs form a ribonucleoprotein complex to recycle stalled ribosomes by
9 non-stop mRNAs and tag incomplete nascent chains for degradation through the fusion of the
10 SsrA peptide²⁵⁻²⁶. In *E. coli* and related bacteria, this tag sequence is recognized by the
11 endogenous proteases ClpXP and ClpAP (that belong to the proteasome complex), which rapidly
12 degrade the target protein. A separate proteolytic mechanism found in the prokaryotic world is the
13 processing of viral poly-proteins. The process is mediated by enzymes that target specific amino
14 acid sequences in otherwise very long polypeptide chains, thereby releasing functional individual
15 proteins. One archetypal example of such poly-protein processing is based on the action of the
16 so-called Nla protease (*nuclear inclusion protein A*)²⁷⁻²⁸. This enzyme was isolated from a virus of
17 the Potyviridae family (positive-sense single-stranded RNA genome) and it has the typical
18 structural motifs of serine proteases—although there is a cysteine residue instead of serine at the
19 active site²⁹⁻³¹. The Nla protease has been used for the proteolytic removal of both affinity tags
20 and fusion proteins from recombinant target proteins, due to the stringent sequence specificity of
21 the proteolytic cleavage (a mere 13 amino acid sequence)³².

22

23 Based on these properties, in this work we present *FENIX* (*f*unctional engineering of SsrA/*Nla*-
24 based flux control), a novel tool that merges the two independent degradation systems mentioned
25 above (i.e. tmRNAs and the Nla protease), for the sake of a rapid and convenient *in vivo* control
26 of protein activities in cell factories. To this end, a synthetic Nla/SsrA tag, which can be easily
27 fused to the C-terminal region of any given protein *via* a single cloning step in a standardized
28 vector, was engineered to include sequences recognized by both the protease and the
29 proteasome. Unlike other systems for post-transcriptional regulation, the strategy relies on the
30 constitutive degradation of the target followed by its conditional restoration. This system was

1 instrumental to bring about an efficient decoupling of PHB accumulation from bacterial growth in
2 recombinant *E. coli* strains by targeting a key enzyme of the PHA biosynthesis machinery.

3

4 **RESULTS AND DISCUSSION**

5

6 **Rationale of *FENIX*, a synthetic post-translational control system for pathway engineering.**

7 In this work, a novel regulatory system at the post-translational level is presented that repurposes
8 the bacterial proteasome and combines its action with the specific protease Nla, the activity of
9 which can be externally controlled at the user's will. While typical control devices based on
10 proteolysis eliminate specific target proteins³³⁻³⁵, the *FENIX* system presented herein is based in
11 just the i.e. the target is constitutively degraded by default by the endogenous proteasome until
12 the conditional activity of the Nla protease removes the degradation signals and enables
13 accumulation of the protein of interest (Fig. 1). To this end a synthetic tag sequence was
14 designed where the recognition sequence of the potyvirus Nla protease (GESNVVHQADER)
15 was fused to the SsrA target sequence (AANDENYALAA) recognized by the ClpXP and ClpAP
16 components of the bacterial proteasome³⁶. The synthetic Nla/SsrA tag
17 (GESNVVHQADER·AANDENYALAA) can be directly fused to the C-terminal domain of virtually
18 any protein, rendering the polypeptide sensitive to rapid degradation by the proteasome system
19 and abolishing the protein accumulation and/or activity (Fig. 1a). In the presence of the Nla
20 protease, in contrast, the proteolytic activity cleaves off the Nla/SsrA tag between the Q and A
21 residues of the tagged polypeptide, which will then releases the SsrA target sequence from the C-
22 terminus, thereby allowing for protein accumulation and/or enzyme activity (Fig. 1a).

23

24 In order to implement this scheme, a novel set of plasmids, based on the structure set by the
25 *Standard European Vector Architecture*³⁷⁻³⁸, was constructed to facilitate the direct tagging of
26 virtually any protein sequence with the synthetic Nla/SsrA tag (Fig. 1b; see details in *Methods*).
27 *FENIX* vectors allow for the easy exchange of the gene encoding a fluorescent protein with the
28 coding sequence of the protein of interest upon digestion and ligation with the unique enzyme
29 cutters *NheI* and *BsrGI* (Table 1). The resulting *FENIX* plasmid will thus express a *nialssrA*
30 tagged version of the gene of interest under the transcriptional control of the constitutive P_{tetA}
31 promoter. An auxiliary plasmid, termed pS238-Nla, was also constructed for the regulatable

1 expression of the gene encoding the Nla protease by placing the cognate coding sequence under
2 the transcriptional control of the *XylS/Pm* expression system (Table 1), inducible upon addition of
3 3-methylbenzoate (3-mBz). With these plasmids at hand, we set out to calibrate the *FENIX*
4 system as indicated in the next section.

5

6 The *FENIX* system enables precise control of protein accumulation in recombinant *E. coli*
7 strains. Our first attempts at calibrating the *FENIX* system involved two fluorescent reporter
8 proteins, the commonly-used green fluorescent protein (GFP) and the red fluorescent protein
9 mCherry, which have been individually fused to the synthetic *nial/ssrA* tag in plasmids
10 pFENIX-*gfp** and pFENIX-*mCherry** [Table 1; note that the asterisk symbol (*) indicates the
11 addition of the synthetic Nla/SsrA tag to the corresponding polypeptide]. Each plasmid was
12 separately transformed along with plasmid pS238-Nla in *E. coli* DH10B. When either GFP* or
13 mCherry* are produced in *E. coli*, they will be rapidly degraded by the proteasome, i.e. no green
14 or red fluorescence is to be seen under these conditions. Inspection of the plates in which the *E.*
15 *coli* recombinants were streaked under blue light indicated that this was the case, as the colonies
16 had no visually-detectable fluorescence (data not shown). In these strains, inducing the
17 expression of *nial* from plasmid pS238-Nla would ultimately result in the removal of the SsrA tag,
18 and the proteasome would no longer be able to degrade the fluorescent proteins, which could
19 thus be detected once they accumulate in the cells at sufficient levels. To explore the kinetic
20 properties of the *FENIX* system, these recombinant *E. coli* strains were grown in multi-well
21 microtiter plates in LB medium with the antibiotics and additives (3-mBz) indicated in *Methods*,
22 and bacterial growth and fluorescence (GFP or mCherry) were recorded after 24 h of incubation
23 at 37°C (Fig. 2).

24

25 The results of population-level fluorescence indicated that the qualitative behavior of the *FENIX*
26 system was reproducible irrespective of nature of the tagged fluorescent protein. When the
27 tagged GFP* or mCherry* proteins were exposed to the action of the Nla protease, the levels of
28 fluorescence attained after 24 h of cultivation were comparable to those observed in the positive
29 controls, in which the genes encoding the native (i.e. non-tagged) GFP or mCherry proteins were
30 constitutively expressed from the *P_{letA}* promoter (Fig. 2). In the case of GFP*, the final
31 fluorescence levels were ca. 70% of those observed for GFP; for mCherry*, the fluorescence

1 output was ca. 90% of that observed for the non-tagged version of the protein. The *FENIX* system
2 also exhibited remarkably low levels of either GFP* or mCherry* fluorescence in the absence of
3 3-mBz, which indicates that the (potential) leaky expression of *nla* does not significantly affect the
4 output fluorescence (i.e. < 10% of the fluorescence levels observed upon induction of the system
5 in both cases)—thereby enabling tight control of protein accumulation. Moreover, and in order to
6 explore the possible effects of the inducer of *nla* expression (3-mBz) on the behavior of the
7 system, we also measured the specific fluorescence in cultures of *E. coli* harboring only plasmids
8 pFENIX-*gfp** or pFENIX-*mCherry** in the presence or the absence of 3-mBz. As indicated in Fig.
9 2, the levels of specific fluorescence in either case were as low as the negative control (i.e. no
10 fluorescent protein), irrespective of the presence of 3-mBz. These quantitative results were
11 mirrored by the fluorescence observed in bacterial pellets of the recombinants harvested from
12 shaken-flask cultures grown under the same conditions (Fig. 2, lower panel). Taken together,
13 these results demonstrate that the *FENIX* system is functional in *E. coli* under the conditions
14 tested, and that the proposed strategy can be established as a model for synthetic post-
15 translational regulation. The next relevant question was to address the kinetic behavior of the
16 system by means of flow cytometry.

17

18 The *FENIX* system enables a precise and concerted temporal switch of protein
19 accumulation. Since the experiments described in the preceding section analyzed the behavior
20 of the *FENIX* system at the whole-population level, we decided to use *E. coli* DH10B transformed
21 both with plasmid pS238-*Nla* and plasmid pFENIX-*gfp** in a set of experiments aimed at an in-
22 depth characterization of the *FENIX* system at the single-cell level (Fig. 3). In this case, the
23 recombinants were grown in LB medium in shaken-flask cultures under the same culture
24 conditions used in the experiments carried out in microtiter-plate cultures, and samples were
25 periodically taken to analyze the levels of GFP* fluorescence by flow cytometry. At the first data
26 point, taken at 3 h post-induction of the system by the addition of 3-mBz at 1 mM, the induced
27 (i.e. GFP*-positive) bacterial culture behaved as a single population (i.e. characterized by a single
28 peak in the histogram plot of cell count *versus* GFP* fluorescence; Fig. 3a, first panel), clearly
29 distinguishable from the non-induced bacterial population (i.e. cultures grown in the absence of 3-
30 mBz). This observation indicates that the operation of the *FENIX* system does not result in a
31 mixture of sub-populations of induced and non-induced cells. The level of GFP* fluorescence

1 rapidly increased after 5 and 8 h post-induction (Fig. 3a, second and third panel) and plateaued
2 at 24 h (Fig. 3a, fourth panel) at fluorescence values slightly below those observed in the positive
3 control (i.e. *E. coli* DH10B transformed with plasmid pS341T·*gfp**, which constitutively expresses
4 a GFP variant displaying exactly the same amino acid sequence of the Nla/SsrA-tagged GFP
5 after digestion by the Nla protease; see *Methods* for details on the construction). Interestingly, the
6 non-induced cultures exhibited levels of GFP* fluorescence within the range of the strain used as
7 a negative control (i.e. *E. coli* DH10B transformed with plasmid pS238·Nla) throughout the whole
8 cultivation period—thus indicating a very low level of leakiness of the *FENIX* system in the
9 absence of any inducer.

10

11 When the induction levels were calculated in this experiment (i.e. GFP* fluorescence in cells from
12 induced cultures as compared to those in the non-induced control experiments), a linear increase
13 in the fluorescence fold-change was observed over time (Fig. 3b). By the end of the experiment
14 (i.e. 24 h post-induction with 3-mBz), the GFP* fluorescence levels in cultures of *E. coli* DH10B
15 transformed both with plasmids pS238·Nla and pFENIX·*gfp** was 24-fold higher than those
16 observed in the non-induced cultures of the same strain (and ca. 60-fold higher than those in
17 cultures of *E. coli* DH10B transformed only with plasmid pS238·Nla, used as the negative control
18 in these experiments). These results accredit the versatility of the *FENIX* system to externally
19 control the accumulation of a target protein in a tightly regulated, and temporally coordinated
20 fashion. Once the calibration of the system was complete, we exploited *FENIX* for tackling a
21 longstanding problem in metabolic engineering of biopolymers as disclosed below.

22

23 **Establishing a *FENIX*-based metabolic switch for biopolymer accumulation in recombinant**
24 ***E. coli* strains.** *E. coli* is a suitable host for engineering biopolymer biosynthesis as it lacks the
25 machinery needed for PHA accumulation and degradation³⁹, offering the flexibility to manipulate
26 both native and heterologous pathways for biopolymer production⁴⁰. PHAs are ubiquitous
27 polymers that attract increasing industrial interest as renewable, biodegradable, biocompatible,
28 and versatile thermoplastics⁴¹. Poly(3-hydroxybutyrate) (PHB) is the structurally simplest and
29 most widespread example of PHA in which the polymer is composed by C4 (i.e. 3-
30 hydroxybutyrate) units. The archetypal PHB biosynthesis pathway of the Gram-negative
31 bacterium *Cupriavidus necator* comprises three enzymes⁴² that use acetyl-CoA as the precursor

1 and NADPH as the redox cofactor (Fig. 4a). PhaA, a 3-ketoacyl-CoA thiolase, condenses two
2 acetyl-CoA moieties to yield 3-acetoacetyl-CoA. This intermediate is the substrate for PhaB1, a
3 NADPH-dependent 3-acetoacetyl-CoA reductase. In the final step, (*R*)-(-)-3-hydroxybutyryl-CoA
4 is polymerized to PHB by the PhaC1 short-chain-length PHA synthase. Expression of the
5 *phaC1AB1* gene cluster from *C. necator* in *E. coli* results in the glucose-dependent accumulation
6 of PHB, and several examples of metabolic engineering of biopolymer accumulation have been
7 published over the last few decades¹⁸⁻²⁰. Yet, the spatiotemporal control of biopolymer
8 accumulation continues to prove challenging. On one hand, draining of acetyl-CoA away from
9 central carbon metabolism interferes with bacterial growth if the PHB biosynthetic pathway is
10 expressed during the active growth phase. On the other hand, acetyl-CoA is a hub metabolite in
11 the cell, used as a precursor by a large number of metabolic pathways, and achieving precursor
12 levels leading to high levels of PHB accumulation is inherently difficult considering the number of
13 competing routes that also use acetyl-CoA. We hypothesized that the efficient uncoupling of
14 bacterial growth and biopolymer accumulation could be an alternative for efficient PHB
15 biosynthesis. Accordingly, the *FENIX* system was adapted to artificially control the level (and
16 hence, the activity) of PhaA, the first committed step of the PHB biosynthesis pathway—and
17 bottleneck of the entire route⁴³—at the post-translational level in recombinant *E. coli* strains (Fig.
18 4b). In order to tackle this challenge, *phaA*, the second gene in the *phaC1AB1* gene cluster, was
19 added with the synthetic *nia/ssrA* tag fragment in the 3'-end of the coding sequence (i.e. C-
20 terminal domain of the protein) as indicated in *Methods*. The resulting engineered protein, PhaA*,
21 would be constitutively degraded by the bacterial proteasome unless the activity of the Nla
22 protease removes the SsrA tag from the polypeptide. On this background, the synthetic metabolic
23 switch for controlled PHB accumulation based on the *FENIX* system was characterized as
24 indicated in the next section.

25

26 The PhaA activity can be tightly regulated by means of the *FENIX* system. *E. coli* BW25113,
27 a well characterized wild-type strain⁴⁴, was transformed with plasmids pS238-Nla and
28 pFENIX-PHA* (Table 1). Plasmid pFENIX-PHA* expresses the *phaC1AB1* gene cluster of *C.*
29 *necator* from its own constitutive promoter, and contains a variant of *phaA* fused to the *nia/ssrA*-
30 tag sequence (Fig. 4b). Shaken-flask cultures of this recombinant strain were carried out in LB
31 medium containing 30 g L⁻¹ glucose, and growth parameters, PHB accumulation and the *in vitro*

1 PhaA activity were periodically monitored over 24 h (Fig. 5). We first explored if the PhaA activity
2 can be switched on by means of the *FENIX* system. In non-induced cultures (i.e. without addition
3 of 3-mBz), the levels of 3-ketoacyl-CoA thiolase activity consistently remained below $2 \mu\text{mol min}^{-1}$
4 $\text{mg}_{\text{protein}}^{-1}$ throughout the cultivation (Fig. 5a). This background thiolase activity was also detected
5 in *E. coli* BW25113 transformed only with plasmid pS238-NIa, and can be accounted for by the
6 endogenous ketoacyl-CoA thiolases of *E. coli* (e.g. AtoB and FadA). In contrast, when 3-mBz was
7 added to the cultures at 1 mM, a quick and sharp increase in the *in vitro* PhaA activity was
8 detected, reaching a 30-fold higher level at 8 h post-induction. By 24 h of cultivation, the PhaA
9 activity in induced cultures had reached $6.1 \pm 0.7 \mu\text{mol min}^{-1} \text{mg}_{\text{protein}}^{-1}$. In a parallel experiment,
10 *E. coli* BW25113/pS238-NIa was transformed either with plasmids pAeT41 or pS341-PHA, which
11 constitutively express the native *phaC1AB1* gene cluster of *C. necator* (in the latter case, in the
12 same vector backbone used for FENIX plasmids, i.e. pSEVA341). The *in vitro* PhaA activity was
13 measured in 24-h cultures of these recombinant strains under the same growth conditions
14 indicated above, in the absence of presence of 3-mBz (Fig. 5b). *E. coli* BW25113/pS238-NIa
15 transformed either with plasmids pAeT41 or pS341-PHA had similarly high levels of PhaA activity
16 irrespective of the presence of 3-mBz. In contrast, a clear difference in the thiolase activity was
17 detected in *E. coli* BW25113 transformed both with plasmids pS238-NIa and pFENIX-PHA*. In
18 non-induced cultures, the enzymatic activity remained at levels $< 1 \mu\text{mol min}^{-1} \text{mg protein}^{-1}$ even
19 after 24 h of cultivation, but the addition of 3-mBz triggered an 8-fold increase in PhaA activity.
20 Moreover, the activity in the induced cultures carrying the PhaA* variant reached the highest
21 levels among all experimental strains and conditions. The tighter control of protein accumulation
22 afforded by the *FENIX* system thus contributes to 1.6-fold higher activity levels of the tagged
23 enzyme as compared to the native PhaA.

24

25 The levels of PHB accumulation were also inspected in these cultures by means of flow
26 cytometry and gas chromatography as indicated in *Methods*. The content of PHB in the bacterial
27 biomass closely mirrored the levels of PhaA activity in all recombinants (Fig. 5c). Again, 3-mBz-
28 induced cultures of the strain carrying the NIa/SsrA-tagged variant of PhaA exhibited the highest
29 polymer content on a cell dry weight (CDW) basis [$56.2\% \pm 6.1\%$ (w/w), 7-fold higher than that in
30 non-induced cultures] among all strains tested. Importantly, all the strains grew at similar levels
31 (with a final biomass density of ca. $5 \text{g}_{\text{CDW}} \text{L}^{-1}$ at 24 h), indicating that the differences observed in

1 PHB accumulation across the recombinants can be attributed to the dynamics of PhaA* activity
2 brought about by the *FENIX* system and not to any effect on bacterial growth.

3

4 **The *FENIX* system enables efficient decoupling of PHB biosynthesis and bacterial growth**
5 **and leads to high rates of biopolymer accumulation.** In order to gain further insights into the
6 dynamics of PHB accumulation in our recombinant *E. coli* strains in shaken-flask cultures, we
7 carried out a thorough physiological characterization in M9 minimal medium containing 30 g L⁻¹
8 glucose as the sole carbon source (Fig. 6). To this end, bacterial growth and PHB accumulation
9 were closely monitored over 24 h in batch cultures of *E. coli* BW25113/pS238-N1a carrying either
10 plasmid pS341-PHA (native PhaA) or pFENIX-PHA* (N1a/SsrA-tagged PhaA). The growth of the
11 two strains was comparable, and the final biomass density plateaued at ca. 3.5 g_{CDW} L⁻¹ (Fig. 6a).
12 The trajectory of PHB accumulation, in contrast, differed between the two strains (Fig. 6b). In *E.*
13 *coli* BW25113/pS238-N1a carrying pS341-PHA, the amount of PHB increased exponentially
14 throughout the cultivation period (i.e. closely resembling biomass formation), whereas in the
15 strain carrying the PhaA* variant the accumulation of PHB was clearly dissociated from bacterial
16 growth, consistently < 5% (w/w) during the first 8 h of cultivation. Once PHB accumulation was
17 triggered, it rapidly increased exponentially. Similarly to the observation made in LB cultures, the
18 strain carrying the N1a/SsrA-tagged version of PhaA attained a higher PHB content in these
19 glucose cultures [72.4% ± 1.8% (w/w), 1.3-fold higher than that in the strain expressing the native
20 *phaCTAB1* gene cluster; Fig. 6b].

21

22 Next, we assessed the specific rate of bacterial growth and biopolymer accumulation (Fig. 6c).
23 The specific growth rate (μ), as inferred from the growth curves, was not significantly different
24 between the two *E. coli* recombinants (ca. 0.3 h⁻¹). However, the clear decoupling of PHB
25 accumulation from bacterial growth in the strain carrying the PhaA* variant resulted a 2-fold
26 higher specific rate of PHB accumulation (r_{PHB}). Under these experimental conditions, $r_{\text{PHB}} = 0.41$
27 ± 0.02 h⁻¹, which is the highest reported in the literature for recombinant *E. coli* strains. The
28 growth decoupling effect was also visually evidenced when cells were sampled from these
29 cultures, stained with the lipophilic Nile Red dye, and observed under the fluorescence
30 microscope (Fig. 6d). Upon induction of the *FENIX* system, the rapid accumulation of PHB in the
31 recombinants could be clearly detected as the polymer granules started to fill the bacterial

1 cytoplasm. Taken together, these results suggest that the *FENIX* system can be used as a
2 metabolic switch operating at the acetyl-CoA metabolic node—a possibility that was explored in
3 detail as explained below.

4

5 **Enhanced PHB accumulation mediated by PhaA* stems from flux re-wiring around the**
6 **acetyl-CoA node.** As indicated previously, acetyl-CoA is a metabolic hub in the cell. In the *E. coli*
7 recombinants described in this work, a major competition occurs at this node between the PHB
8 biosynthesis pathway and other endogenous metabolic routes. Apart from the core cell functions
9 that use acetyl-CoA as building-block (e.g. *de novo* fatty acid synthesis), in the presence of
10 excess glucose, *E. coli* synthesizes (and excretes) acetate from acetyl-CoA through a two-step
11 route catalyzed by Pta (phosphotransacetylase) and AckA (acetate kinase)⁴⁵ (Fig. 7a). Taking
12 advantage of this biochemical feature, we adopted the specific rate of acetate formation and the
13 content of acetyl-CoA as a proxy to gauge how the *FENIX* system could re-direct this metabolic
14 precursor into a target pathway. A lower specific rate of acetate formation was detected in
15 glucose cultures of all *E. coli* strains expressing the PHB biosynthesis pathway as compared to
16 the control strain, transformed with the empty pSEVA341 vector (Fig. 7b)—consistent with a
17 higher flux of acetyl-CoA going into PHB formation. However, *E. coli* BW25113/pS238-Nla
18 transformed with plasmid pFENIX-PHA* had the lowest rate of acetate synthesis along all the
19 strains tested (0.9 ± 0.1 mmol g_{CDW}⁻¹ h⁻¹; 70% lower than that of the control strain). Interestingly,
20 when the specific rates of glucose consumption were also determined in these cultures, no major
21 differences were observed among all the strains (with q_s values around 7-8 mmol g_{CDW}⁻¹ h⁻¹),
22 indicating that the differences in acetate formation or PHB accumulation are linked to a re-routing
23 of acetyl-CoA rather than to significant changes in the overall cell physiology.

24

25 The intracellular acetyl-CoA content qualitatively followed the same trend as the specific rates of
26 acetate formation, although the values obtained for this parameter were comparable among the
27 control strain and the *E. coli* recombinants expressing the native *phaC1AB1* gene cluster (Fig.
28 7c). Again, the tight control of the PHB biosynthesis pathway at the level of PhaA afforded by the
29 *FENIX* system was reflected in the lowest content of acetyl-CoA among all the strains tested
30 (0.23 ± 0.05 nmol g_{CDW}⁻¹)—suggesting an efficient re-routing of this metabolic precursor into PHB
31 accumulation rather than into other metabolic sinks of acetyl-CoA. These results accredit that the

1 *FENIX* system could be used to establish an orthogonal control over key metabolic nodes in the
2 biochemical network, acting as a switch to re-route the fluxes around such nodes towards the
3 formation a product of interest.

4

5 CONCLUSION

6

7 So far, re-programming microorganisms to modify existing cell functions and to bestow bacterial
8 cell factories with new-to-Nature tasks have largely relied on the implementation of specialized
9 molecular biology tools—which, for the most part, tackle the issue at the genetic level of
10 regulation. More recently, novel approaches for pathway engineering also encompass dynamic
11 regulation of protein levels. *FENIX* exploits a hitherto unexplored feature, namely, the constitutive
12 degradation of a target protein within a pathway, the accumulation of which can be triggered at
13 the user's will by addition of a cheap inducer (i.e. 3-mBz) to the culture medium. Besides the
14 metabolic engineering application discussed in the present study (i.e. biopolymer accumulation in
15 recombinant *E. coli* strains by targeting PhaA, the first enzymatic activity of the pathway), the
16 *FENIX* system affords more complex pathway engineering approaches in which the formation of
17 multiple proteins within different domains of the metabolic network can be externally controlled.
18 The tight post-translational regulation of the system enables product titers that would be difficult
19 to achieve by merely manipulating the level of expression of the cognate genes. Moreover, and
20 considering the dynamic response of *FENIX*-tagged proteins accumulation, the system would
21 also allow for the expression of highly toxic proteins or enzymes. These scenarios are currently
22 under exploration in our laboratory and may lead to the development of better strategies to
23 manipulate central and peripheral pathways to enhance the production of biochemicals and other
24 molecules of industrial interest.

25

26 METHODS

27

28 **Bacterial strains and cultivation conditions.** The *E. coli* strains and plasmids used in this study
29 are listed in Table 1. *E. coli* was grown at 37°C in LB medium⁴⁶ or in M9 minimal medium⁴⁷ added
30 with glucose (30 g L⁻¹) as the sole carbon source. For solidified culture media, 1.5% (w/v) agar
31 was used. Shaken-flask cultivations were routinely carried out in an air incubator with orbital

1 shaking at 200 rpm. Aerobic cultures were set by using a 1:10 culture medium-to-flask volume
2 ratio. Antibiotics were added to the cultures where appropriate at the following final
3 concentrations: ampicillin (Ap, 150 mg L⁻¹), chloramphenicol (Cm, 30 mg L⁻¹), and kanamycin
4 (Km, 50 mg L⁻¹).

5

6 **General molecular biology techniques.** Recombinant DNA techniques were carried out by
7 following well established methods⁴⁸. Plasmid DNA was prepared from *E. coli* recombinants with
8 a High-Pure plasmid isolation kit (Roche Applied Science). DNA fragments were purified from
9 agarose gels with the Gene-Clean Turbo kit (Q-BIOgene). Oligonucleotides were purchased from
10 Sigma-Aldrich Co. The identity of all cloned inserts and DNA fragments was confirmed by DNA
11 sequencing through an ABI Prism 377 automated DNA sequencer (Applied Biosystems Inc.).
12 Transformation of *E. coli* cells with plasmids was routinely carried out by means of the RbCl
13 method or by electroporation⁴⁸ (Gene Pulser, Bio-Rad).

14

15 **Design and construction of *FENIX* plasmids carrying proteolizable versions of GFP and**
16 **mCherry.** The general strategy for the assembly of *FENIX* plasmids is indicated in Fig. 1b. In all
17 the constructs described in this article, the asterisk symbol (*) indicates that the corresponding
18 gene has been added with a synthetic *nialssrA* tag. The starting point was the creation of
19 plasmids pFENIX-*gfp** and pFENIX-*mCherry** as follows: the *nialssrA* tag was firstly assembled
20 using the synthetic oligonucleotides 5'-*nialssrA*-*BsrGI* (5'-GAG CTG TAC AAG GGT GAA AGC
21 AAC GTG gtg gtg cat cag gcg gat gaa cgc gca gca aac gac gaa aac-3'; an engineered *BsrGI* site,
22 not present in SEVA vectors³⁷, is underlined) and 3'-*nialssrA*-*HindIII* (5'-CCC AAG CTT TTA AGC
23 TGC TAA AGC GTA gtt ttc gtc gtt tgc tgc gcg ttc atc cgc ctg atg cac cac-3'; an engineered *HindIII*
24 site is underlined). The 42-bp long DNA sequence indicated in lowercase letters in these two
25 oligonucleotides was used as an overlapping extension for sewing PCR, and the whole 89-bp
26 long DNA fragment spanning the synthetic *nialssrA* tag was amplified with *Pfu* DNA polymerase
27 (Promega) as per the manufacturer's instructions. Plasmid pS341T was constructed by cloning
28 the *P_{tetA}* promoter (a medium-strength constitutive promoter in Gram-negative bacteria in the
29 absence of the TetR negative regulator⁴⁹) between the *PadI* and *EcoRI* restriction targets of
30 vector pSEVA341, and a *NheI* restriction target, not present in SEVA vectors, was added to the
31 construct to facilitate further cloning. Plasmid pS341T-*mCherry* was constructed by placing the

1 gene encoding the red fluorescent protein mCherry under control of the P_{tetA} promoter as a
2 *XhoI/HindIII* fragment obtained from vector pSEVA237R, and a *BsrGI* restriction target was added
3 upstream the *mCherry* coding sequence by PCR. The resulting pS341T·*mCherry* plasmid was
4 further engineered to include the synthetic *nial/ssrA* tag by means of sewing PCR. The tag was
5 directly cloned as a *BsrGI/HindIII* fragment downstream the *mCherry* gene, thus giving rise to
6 pFENIX·*mCherry** (Table 1). The same procedure was repeated with the gene encoding GFP,
7 yielding pFENIX·*gfp** (Table 1). Both plasmids were used to calibrate the FENIX system, and
8 they allow for the easy construction of a proteolizable version of virtually any protein by a direct
9 cloning step of the corresponding gene of interest into the *NheI* and *BsrGI* restriction sites that
10 flank the fluorescent protein coding sequence.

11
12 Two expression vectors were also constructed as positive controls of the FENIX system. In order
13 to establish a direct comparison between the fluorescence originated by the engineered GFP* or
14 mCherry* fluorescent proteins after proteolysis, we designed and created a version of these two
15 proteins that have the same amino acid sequence as the proteolizable variants after digestion by
16 the Nla protease. Plasmid pS341T·*mCherry**, encoding such an engineered mCherry protein,
17 was constructed by amplifying the *mCherry* gene plus the short sequence of the *nial* target that
18 remains after protease digestion using oligonucleotides 5'-mCherry·*NheI* (5'-CAC AGG AGG
19 GCT AGC ATG GTG AG-3'; an engineered *NheI* site is underlined) and 3'-*mCherry*·*HindIII* (5'-
20 GGG AAG CTT TTA CTG ATG CAC CAC CAC GTT GCT TTC-3'; an engineered *HindIII* site is
21 underlined) by using plasmid pFENIX·*mCherry** as the template. The resulting amplicon, which
22 spans the sequence encoding the mCherry protein after proteolysis, was restricted with the
23 enzymes indicated and cloned into the *NheI/HindIII*-digested pS341T vector, thereby obtaining
24 plasmid pS341T·*mCherry** (Table 1). The same procedure was repeated for GFP, yielding
25 plasmid pS341T·*gfp** (Table 1).

26
27 Construction of plasmid pFENIX·PHA* for post-translational control of PHB accumulation
28 in recombinant *E. coli* strains. Since *phaA* lies in the middle of the *pha* gene cluster of *C.*
29 *necator*, the strategy used for tagging this gene was slightly different as the one described above
30 for single-gene targets. In this case, the synthetic *nial/ssrA* tag was firstly added to *phaA* by
31 overlapping PCR. Two individual DNA fragments upstream and downstream with respect to the

1 *STOP* codon of *phaA* were amplified by PCR using oligonucleotides (i) 5'-*phaA*·*Bgl*II (5'-CAC
2 GCG GCA AGA TCT CGC AGA CC-3'; an engineered *Bgl*II site is underlined) and 3'-*phaA*·*nia*
3 (5'- cgt cgt ttg ctg cgc gtt cat ccg cct gat gca cca cca cgt tgc ttt cac cTT TGC GCT CGA CTG
4 CCA GCG C-3') for the upstream fragment (2,462 bp) and (ii) 5'-*phaA*·*nia* (5'-gca tca ggc gga tga
5 acg cgc agc aaa cga cga aaa cta cgc ttt agc agc tTA AGG AAG GGG TTT TCC GGG GC-3') and
6 3'-*phaA*·*Eco*RI (5'-GAC CAT GAT TAC GAA TTC TTC TGA ATC CAT G-3'; an engineered *Eco*RI
7 site is underlined) for the downstream fragment (1,398 bp). Both amplicons were used to
8 construct a DNA fragment spanning *phaA* and the synthetic *nia/ssrA* tag by sewing PCR using
9 the overlapping sequences in the oligonucleotides 5'-*phaA*·*nia* and 3'-*phaA*·*nia* (indicated in
10 lowercase letters). This DNA fragment was cloned into the *Bgl*II/*Eco*RI-digested plasmid pAET41,
11 obtaining plasmid pAeT41·PHA*, in which the native *phaA* sequence has been exchanged by the
12 *nia/ssrA* tagged version of the same gene. Plasmid pAeT41·PHA* was then used as the template
13 for a PCR amplification of the engineered *pha* gene cluster by using oligonucleotides 5'-
14 PHA·*Bam*HI (5'-AGA GGA TCC GGA CTC AAA TGT CTC GGA ATC GCT G-3'; an engineered
15 *Bam*HI site is underlined) and 3'-PHA·*Eco*RI (5'-GCG AAT TCC ACC GCA ATA CGC GGG CGC
16 CAG-3'; an engineered *Eco*RI site is underlined). The resulting amplicon (4,292 bp) was digested
17 with *Bam*HI and *Eco*RI and cloned into the same restriction sites of vector pSEVA341, resulting in
18 plasmid pFENIX·PHA*. To test PHB accumulation using a comparable vector system, plasmid
19 pS341·PHA was constructed as follows. The native *pha* gene cluster was amplified by PCR from
20 plasmid pAeT41 as the template using oligonucleotides 5'-PHA·*Bam*HI and 3'-PHA·*Eco*RI. The
21 resulting DNA fragment (4,220 bp) was digested with *Bam*HI and *Eco*RI and cloned into the same
22 restriction sites of vector pSEVA341, resulting in plasmid pS341·PHA. *E. coli* BW25113 was
23 transformed with plasmid pS238·Nla and either pS341·PHA or pFENIX·PHA*, and tested for PHB
24 accumulation as indicated below.

25

26 Flow cytometry evaluation of the *FENIX* system. Single-cell fluorescence was analyzed with a
27 MACSQuant™ VYB cytometer (Miltenyi Biotec GmbH). GFP was excited at 488 nm, and the
28 fluorescence signal was recovered with a 525/40 nm band pass filter. Cells were harvested at
29 different time points as indicated in the text, and at least 15,000 events were analyzed for every
30 aliquot. The GFP signal was quantified under the experimental conditions tested by firstly gating
31 the cells in a side scatter against forward scatter plot, and then the GFP-associated fluorescence

1 was recorded in the FL1 channel (515-545 nm). Data processing was performed using the
2 FlowJo™ software as described elsewhere⁵⁰.

3

4 ***In vitro* quantification of the PhaA activity.** Cell-free extracts were obtained from bacteria
5 harvested by centrifugation (4,000×*g* at 4°C for 10 min). Cell pellets were resuspended in 1 mL of
6 a lysis buffer containing 10 mM Tris·HCl (pH = 8.1), 1 mM EDTA, 10 mM β-mercaptoethanol,
7 20% (v/v) glycerol, and 0.2 mM phenylmethylsulphonylfluoride, and lysed as described
8 elsewhere⁵¹. The lysate was clarified by centrifugation (4°C, 10 min at 8,000×*g*) and the resulting
9 supernatant was used for enzyme assays. The total protein concentration was assessed by
10 means of the Bradford method with a kit from BioRad Laboratories, Inc. (USA), and crystalline
11 bovine serum albumin as standard. *In vitro* quantification of the specific 3-ketoacyl-CoA thiolase
12 activity in the thiolysis direction was conducted according to Palmer et al.⁵² and Slater et al.⁴²,
13 with the following modifications. The assay mixture (1 mL) contained 62.4 mM Tris·HCl (pH =
14 8.1), 50 mM MgCl₂, 62.5 μM CoA, and 62.5 μM acetoacetyl-CoA. The reaction was initiated by
15 addition of cell-free extract, and the disappearance of acetoacetyl-CoA was measured over time
16 at 30°C (using $\epsilon_{304} = 16.9 \times 10^3 \text{ M}^{-1} \text{ cm}^{-1}$ as the extinction coefficient for 3-acetoacetyl-CoA). The
17 actual acetoacetyl-CoA was routinely quantified prior to the assay in a buffer containing 62.4 mM
18 Tris·HCl (pH = 8.1) and 50 mM MgCl₂. One enzyme unit is defined as the amount of enzyme
19 catalyzing the conversion of 1 μmol of substrate per min at 30°C.

20

21 **PHB quantification.** The intracellular polymer content in *E. coli* was quantitatively assessed by
22 flow cytometry by using a slight modification of the protocol of Tyo et al.⁵³ and Martínez-García et
23 al.⁵⁴ Cultures were promptly cooled to 4°C by placing them in an ice bath for 15 min. Cells were
24 harvested by centrifugation (5 min, 5,000×*g*, 4°C), resuspended to an OD₆₀₀ of 0.4 in cold TES
25 buffer [10 mM Tris·HCl (pH = 7.5), 2.5 mM EDTA, and 10% (w/v) sucrose], and incubated on ice
26 for 15 min. Bacteria were recovered by centrifugation as explained above, and resuspended in
27 the same volume of cold 1 mM MgCl₂. A 1-ml aliquot of this bacterial suspension was added with
28 3 μL of a 1 mg mL⁻¹ Nile Red [9-diethylamino-5H-benzo(α)phenoxazine-5-one] solution in DMSO
29 and incubated in the dark at 4°C for 30 min. Flow cytometry was carried out in a MACSQuant™
30 VYB cytometer (Miltenyi Biotec GmbH). Cells were excited at 488 nm with a diode-pumped solid-
31 state laser, and the Nile Red fluorescence at 585 nm was detected with a 610 nm long band-pass

1 filter. The analysis was done on at least 50,000 cells and the results were analyzed with the built-
2 in MACSQuantify™ software 2.5 (Miltenyi Biotec). The geometric mean of fluorescence in each
3 sample was correlated to PHB content (expressed as a percentage) through a calibration curve.
4 PHB accumulation was double-checked in selected samples by acid-catalyzed methanolysis of
5 freeze-dried biomass and detection of the resulting methyl-esters of 3-hydroxybutyric acid by gas
6 chromatography^{23, 55-56}.

7
8 For microscopic visualization of PHB accumulation⁵⁷, cells harvested from shaken-flask cultures
9 were washed once with cold TES buffer, re-suspended in 1 mL of the same buffer to an OD₆₀₀ of
10 0.4, and stained with Nile Red as indicated for the flow cytometry experiments. Aliquots of the
11 treated cell suspension were washed once with TES buffer, immediately lay in a microscope
12 slide, and covered with a glass cover slip (to protect the stained cells from immersion oil). Images
13 were obtained using an Axio Imager Z2 microscope (Carl Zeiss), equipped with the scanning
14 platform Metafer 4 and CoolCube 1 camera (MetaSystems) under a 1,000× magnification. Under
15 these conditions, PHB granules stained with Nile Red fluoresced bright orange, with individual
16 granules often visible within the cells.

17
18 **Other analytical techniques.** Residual glucose and acetate concentrations were determined in
19 culture supernatants using enzymatic kits (R-Biopharm AG), essentially as per the manufacturer's
20 instructions. Control mock assays were made by spiking M9 minimal medium with different
21 amounts of the metabolite under examination. Metabolite yields and kinetic culture parameters
22 were analytically calculated from the raw growth data as described elsewhere⁵¹. The intracellular
23 content of acetyl-CoA was determined by liquid chromatography coupled to mass spectrometry
24 as indicated by Pflüger-Grau et al.⁵⁸.

25
26 **Statistical analysis.** All reported experiments were independently repeated at least three times
27 (as indicated in the figure legends), and mean values of the corresponding parameter and
28 standard deviation is presented. The significance of differences when comparing results was
29 evaluated by means of the Student's *t* test.

30

1 **COMPETING INTERESTS**

2 The authors declare that there are no competing interests.

3

4 **AUTHORS' CONTRIBUTIONS**

5 G.D.R. and P.I.N. carried out the genetic manipulations, quantitative physiology experiments, and
6 *in vitro* enzyme assays. G.D.R., V.D.L., and P.I.N. conceived the whole study, designed the
7 experiments, contributed to the discussion of the research and interpretation of the data, and
8 wrote the article.

9

10 **ACKNOWLEDGMENTS**

11 The authors are indebted to B. Calles (CNB-CSIC, Spain), M. H. Nørholm (Technical University of
12 Denmark, Denmark), and A. Sinskey (Massachusetts Institute of Technology, USA) for helpful
13 discussions and for sharing research materials. This study was supported by The Novo Nordisk
14 Foundation (Grant NNF10CC1016517) and the Danish Council for Independent Research
15 (*SWEET*, DFF-Research Project 8021-00039B) to P.I.N. This study was also supported by the
16 *HELIOS* Project of the Spanish Ministry of Economy and Competitiveness BIO2015-66960-C3-2-
17 R (MINECO/FEDER), and the *ARISYS* (ERC-2012-ADG-322797), *EmPowerPutida* (EUH2020-
18 BIOTEC-2014-2015-6335536), and *MADONNA* (H2020-FET-OPEN-RIA-2017-1-766975)
19 contracts of the European Union to V.D.L.

20

21 **REFERENCES**

22

- 23 1. Avcilar-Kucukgoze, I.; Ignatova, Z., Rewiring host activities for synthetic circuit production:
24 a translation view. *Biotechnol. Lett.* **2017**, *39*(1), 25-31.
- 25 2. Wu, G.; Yan, Q.; Jones, J. A.; Tang, Y. J.; Fong, S. S.; Koffas, M. A. G., Metabolic burden:
26 cornerstones in synthetic biology and metabolic engineering applications. *Trends*
27 *Biotechnol.* **2016**, *34*(8), 652-664.
- 28 3. Guzmán, L. M.; Belin, D.; Carson, M. J.; Beckwith, J., Tight regulation, modulation, and
29 high-level expression by vectors containing the arabinose P_{BAD} promoter. *J. Bacteriol.*
30 **1995**, *177*(14), 4121-4130.

- 1 4. Isaacs, F. J.; Dwyer, D. J.; Ding, C.; Pervouchine, D. D.; Cantor, C. R.; Collins, J. J.,
2 Engineered riboregulators enable post-transcriptional control of gene expression. *Nat.*
3 *Biotechnol.* 2004, 22(7), 841-7.
- 4 5. Lou, C.; Stanton, B.; Chen, Y. J.; Munsky, B.; Voigt, C. A., Ribozyme-based insulator parts
5 buffer synthetic circuits from genetic context. *Nat. Biotechnol.* 2012, 30(11), 1137-42.
- 6 6. Lutz, R.; Bujard, H., Independent and tight regulation of transcriptional units in *Escherichia*
7 *coli* via the LacR/O, the TetR/O and AraC/I1-I2 regulatory elements. *Nucleic Acids Res.*
8 1997, 25(6), 1203-10.
- 9 7. Jakočiūnas, T.; Jensen, M. K.; Keasling, J. D., System-level perturbations of cell
10 metabolism using CRISPR/Cas9. *Curr. Opin. Biotechnol.* 2017, 46, 134-140.
- 11 8. Shabestary, K.; Anfelt, J.; Ljungqvist, E.; Jahn, M.; Yao, L.; Hudson, E. P., Targeted
12 repression of essential genes to arrest growth and increase carbon partitioning and biofuel
13 titers in cyanobacteria. *ACS Synth. Biol.* 2018, 7(7), 1669-1675.
- 14 9. Tan, S. Z.; Prather, K. L., Dynamic pathway regulation: Recent advances and methods of
15 construction. *Curr. Opin. Chem. Biol.* 2017, 41, 28-35.
- 16 10. Bonger, K. M.; Chen, L. C.; Liu, C. W.; Wandless, T. J., Small-molecule displacement of a
17 cryptic degron causes conditional protein degradation. *Nat. Chem. Biol.* 2011, 7(8), 531-7.
- 18 11. Janssen, B. D.; Hayes, C. S., The tmRNA ribosome-rescue system. *Adv. Protein Chem.*
19 *Struct. Biol.* 2012, 86, 151-91.
- 20 12. Neklesa, T. K.; Tae, H. S.; Schneekloth, A. R.; Stulberg, M. J.; Corson, T. W.; Sundberg, T.
21 B.; Raina, K.; Holley, S. A.; Crews, C. M., Small-molecule hydrophobic tagging-induced
22 degradation of *HaloTag* fusion proteins. *Nat. Chem. Biol.* 2011, 7(8), 538-43.
- 23 13. Cameron, D. E.; Collins, J. J., Tunable protein degradation in bacteria. *Nat. Biotechnol.*
24 2014, 32(12), 1276-81.
- 25 14. Martínez, V.; Lauritsen, I.; Hobel, T.; Li, S.; Nielsen, A. T.; Nørholm, M. H. H.,
26 CRISPR/Cas9-based genome editing for simultaneous interference with gene expression
27 and protein stability. *Nucleic Acids Res.* 2017, 45(20), e171.
- 28 15. Stein, V.; Nabi, M.; Alexandrov, K., Ultrasensitive scaffold-dependent protease sensors
29 with large dynamic range. *ACS Synth. Biol.* 2017, 6(7), 1337-1342.
- 30 16. Bothfeld, W.; Kapov, G.; Tyo, K. E. J., A glucose-sensing toggle switch for autonomous,
31 high productivity genetic control. *ACS Synth. Biol.* 2017, 6(7), 1296-1304.

- 1 17. Li, S.; Jendresen, C. B.; Grünberger, A.; Ronda, C.; Jensen, S. I.; Noack, S.; Nielsen, A. T.,
2 Enhanced protein and biochemical production using CRISPRi-based growth switches.
3 *Metab. Eng.* 2016, 38, 274-284.
- 4 18. Gomez, J. G. C.; Méndez, B. S.; Nikel, P. I.; Pettinari, M. J.; Prieto, M. A.; Silva, L. F.,
5 Making green polymers even greener: towards sustainable production of
6 polyhydroxyalkanoates from agroindustrial by-products. In *Advances in Applied*
7 *Biotechnology*, Petre, M., Ed. InTech: Rijeka, Croatia, 2012; pp 41-62.
- 8 19. López, N. I.; Pettinari, M. J.; Nikel, P. I.; Méndez, B. S., Polyhydroxyalkanoates: much more
9 than biodegradable plastics. *Adv. Appl. Microbiol.* 2015, 93, 93-106.
- 10 20. Meng, D. C.; Shen, R.; Yao, H.; Chen, J. C.; Wu, Q.; Chen, G. Q., Engineering the diversity
11 of polyesters. *Curr. Opin. Biotechnol.* 2014, 29, 24-33.
- 12 21. Meng, D. C.; Chen, G. Q., Synthetic biology of polyhydroxyalkanoates (PHA). *Adv.*
13 *Biochem. Eng. Biotechnol.* 2018, 162, 147-174.
- 14 22. Leong, Y. K.; Show, P. L.; Ooi, C. W.; Ling, T. C.; Lan, J. C., Current trends in
15 polyhydroxyalkanoates (PHAs) biosynthesis: insights from the recombinant *Escherichia*
16 *coli*. *Journal of biotechnology* 2014, 180, 52-65.
- 17 23. Nikel, P. I.; Giordano, A. M.; de Almeida, A.; Godoy, M. S.; Pettinari, M. J., Elimination of D-
18 lactate synthesis increases poly(3-hydroxybutyrate) and ethanol synthesis from glycerol
19 and affects cofactor distribution in recombinant *Escherichia coli*. *Appl. Environ. Microbiol.*
20 2010, 76 (22), 7400-6.
- 21 24. Becker, S. H.; Darwin, K. H., Bacterial proteasomes: Mechanistic and functional insights.
22 *Microbiol. Mol. Biol. Rev.* 2017, 81 (1).
- 23 25. Doma, M. K.; Parker, R., RNA quality control in eukaryotes. *Cell* 2007, 131 (4), 660-8.
- 24 26. Shoemaker, C. J.; Eyler, D. E.; Green, R., Dom34:Hbs1 promotes subunit dissociation and
25 peptidyl-tRNA drop-off to initiate no-go decay. *Science* 2010, 330 (6002), 369-72.
- 26 27. Carrington, J. C.; Cary, S. M.; Parks, T. D.; Dougherty, W. G., A second proteinase
27 encoded by a plant potyvirus genome. *EMBO J.* 1989, 8 (2), 365-70.
- 28 28. Verchot, J.; Koonin, E. V.; Carrington, J. C., The 35-kDa protein from the N-terminus of the
29 potyviral polyprotein functions as a third virus-encoded proteinase. *Virology* 1991, 185 (2),
30 527-35.

- 1 29. Gorbalenya, A. E.; Donchenko, A. P.; Blinov, V. M.; Koonin, E. V., Cysteine proteases of
2 positive strand RNA viruses and chymotrypsin-like serine proteases. A distinct protein
3 superfamily with a common structural fold. *FEBS Lett.* 1989, 243 (2), 103-14.
- 4 30. Kim, D. H.; Hwang, D. C.; Kang, B. H.; Lew, J.; Choi, K. Y., Characterization of Nla
5 protease from turnip mosaic potyvirus exhibiting a low-temperature optimum catalytic
6 activity. *Virology* 1996, 221 (1), 245-9.
- 7 31. Kim, D. H.; Hwang, D. C.; Kang, B. H.; Lew, J.; Han, J.; Song, B. D.; Choi, K. Y., Effects of
8 internal cleavages and mutations in the C-terminal region of Nla protease of turnip mosaic
9 potyvirus on the catalytic activity. *Virology* 1996, 226 (2), 183-90.
- 10 32. Stevens, R. C., Design of high-throughput methods of protein production for structural
11 biology. *Structure* 2000, 8 (9), R177-R185.
- 12 33. Stein, V.; Alexandrov, K., Protease-based synthetic sensing and signal amplification. *Proc.*
13 *Natl. Acad. Sci. USA* 2014, 111 (45), 15934-9.
- 14 34. Sekar, K.; Gentile, A. M.; Bostick, J. W.; Tyo, K. E., *N*-Terminal-based targeted, inducible
15 protein degradation in *Escherichia coli*. *PLoS One* 2016, 11 (2), e0149746.
- 16 35. Brockman, I. M.; Prather, K. L. J., Dynamic knockdown of *E. coli* central metabolism for
17 redirecting fluxes of primary metabolites. *Metab. Eng.* 2015, 28, 104-113.
- 18 36. Gottesman, S.; Roche, E.; Zhou, Y.; Sauer, R. T., The ClpXP and ClpAP proteases
19 degrade proteins with carboxy-terminal peptide tails added by the SsrA-tagging system.
20 *Genes Dev.* 1998, 12 (9), 1338-47.
- 21 37. Silva-Rocha, R.; Martínez-García, E.; Calles, B.; Chavarría, M.; Arce-Rodríguez, A.; de las
22 Heras, A.; Páez-Espino, A. D.; Durante-Rodríguez, G.; Kim, J.; Nickel, P. I.; Platero, R.; de
23 Lorenzo, V., The Standard European Vector Architecture (SEVA): a coherent platform for
24 the analysis and deployment of complex prokaryotic phenotypes. *Nucleic Acids Res.* 2013,
25 41 (D1), D666-D675.
- 26 38. Durante-Rodríguez, G.; de Lorenzo, V.; Martínez-García, E., The Standard European
27 Vector Architecture (SEVA) plasmid toolkit. *Methods in molecular biology* 2014, 1149, 469-
28 78.
- 29 39. Li, R.; Zhang, H.; Qi, Q., The production of polyhydroxyalkanoates in recombinant
30 *Escherichia coli*. *Bioresour. Technol.* 2007, 98 (12), 2313-2320.

- 1 40. Egoburo, D. E.; Díaz-Peña, R.; Álvarez, D. S.; Godoy, M. S.; Mezzina, M. P.; Pettinari, M.
2 J., Microbial cell factories *à la carte*: Elimination of global regulators Cra and ArcA
3 generates metabolic backgrounds suitable for the synthesis of bioproducts in *Escherichia*
4 *coli*. *Appl. Environ. Microbiol.* 2018.
- 5 41. Anderson, A. J.; Dawes, E. A., Occurrence, metabolism, metabolic role, and industrial uses
6 of bacterial polyhydroxyalkanoates. *Microbiol. Rev.* 1990, 54 (4), 450-72.
- 7 42. Slater, S.; Houmiel, K. L.; Tran, M.; Mitsky, T. A.; Taylor, N. B.; Padgett, S. R.; Gruys, K.
8 J., Multiple b-ketothiolases mediate poly(b-hydroxyalkanoate) copolymer synthesis in
9 *Ralstonia eutropha*. *J. Bacteriol.* 1998, 180 (8), 1979-87.
- 10 43. van Wegen, R. J.; Lee, S. Y.; Middelberg, A. P. J., Metabolic and kinetic analysis of poly(3-
11 hydroxybutyrate) production by recombinant *Escherichia coli*. *Biotechnol. Bioeng.* 2001, 74
12 (1), 70-81.
- 13 44. Datsenko, K. A.; Wanner, B. L., One-step inactivation of chromosomal genes in
14 *Escherichia coli* K-12 using PCR products. *Proc. Natl. Acad. Sci. USA* 2000, 97, 6640-
15 6645.
- 16 45. Chang, D. E.; Shin, S.; Rhee, J. S.; Pan, J. G., Acetate metabolism in a *pta* mutant of
17 *Escherichia coli* W3110: Importance of maintaining acetyl coenzyme A flux for growth and
18 survival. *J. Bacteriol.* 1999, 181 (21), 6656-6663.
- 19 46. Miller, J. H., *Experiments in molecular genetics*. Cold Spring Harbor Laboratory: Cold
20 Spring Harbor, N.Y., 1972.
- 21 47. Nikel, P. I.; Romero-Campero, F. J.; Zeidman, J. A.; Goñi-Moreno, A.; de Lorenzo, V., The
22 glycerol-dependent metabolic persistence of *Pseudomonas putida* KT2440 reflects the
23 regulatory logic of the GlpR repressor. *mBio* 2015, 6 (2), e00340-15.
- 24 48. Sambrook, J.; Russell, D. W., *Molecular cloning: a laboratory manual*. 3rd ed.; Cold Spring
25 Harbor Laboratory: Cold Spring Harbor, 2001.
- 26 49. Muthukrishnan, A. B.; Kandhavelu, M.; Lloyd-Price, J.; Kudasov, F.; Chowdhury, S.; Yli-
27 Harja, O.; Ribeiro, A. S., Dynamics of transcription driven by the *tetA* promoter, one event
28 at a time, in live *Escherichia coli* cells. *Nucleic Acids Res.* 2012, 40 (17), 8472-83.
- 29 50. Dvořák, P.; Chrást, L.; Nikel, P. I.; Fedr, R.; Soucek, K.; Sedlacková, M.; Chaloupková, R.;
30 de Lorenzo, V.; Prokop, Z.; Damborský, J., Exacerbation of substrate toxicity by IPTG in

- 1 *Escherichia coli* BL21(DE3) carrying a synthetic metabolic pathway. *Microb. Cell Fact.*
2 2015, 14, 201.
- 3 51. Nikel, P. I.; Chavarría, M., Quantitative physiology approaches to understand and optimize
4 reducing power availability in environmental bacteria. In *Hydrocarbon and Lipid*
5 *Microbiology Protocols–Synthetic and Systems Biology - Tools*, McGenity, T. J.; Timmis, K.
6 N.; Nogales-Fernández, B., Eds. Humana Press: Heidelberg, Germany, 2016; pp 39-70.
- 7 52. Palmer, M. A. J.; Differding, E.; Gamboni, R.; Williams, S. F.; Peoples, O. P.; Walsh, C. T.;
8 Sinskey, A. J.; Masamune, S., Biosynthetic thiolase from *Zoogloea ramigera*. Evidence for
9 a mechanism involving Cys-378 as the active site base. *J. Biol. Chem.* 1991, 266 (13),
10 8369-75.
- 11 53. Tyo, K. E.; Zhou, H.; Stephanopoulos, G. N., High-throughput screen for poly-3-
12 hydroxybutyrate in *Escherichia coli* and *Synechocystis* sp. strain PCC6803. *Appl. Environ.*
13 *Microbiol.* 2006, 72 (5), 3412-3417.
- 14 54. Martínez-García, E.; Aparicio, T.; de Lorenzo, V.; Nikel, P. I., New transposon tools tailored
15 for metabolic engineering of Gram-negative microbial cell factories. *Front. Bioeng.*
16 *Biotechnol.* 2014, 2, 46.
- 17 55. Nikel, P. I.; Pettinari, M. J.; Galvagno, M. A.; Méndez, B. S., Poly(3-hydroxybutyrate)
18 synthesis by recombinant *Escherichia coli arcA* mutants in microaerobiosis. *Appl. Environ.*
19 *Microbiol.* 2006, 72 (4), 2614-20.
- 20 56. Ruiz, J. A.; Fernández, R. O.; Nikel, P. I.; Méndez, B. S.; Pettinari, M. J., *dye (arc)* Mutants:
21 insights into an unexplained phenotype and its suppression by the synthesis of poly(3-
22 hydroxybutyrate) in *Escherichia coli* recombinants. *FEMS Microbiol. Lett.* 2006, 258 (1), 55-
23 60.
- 24 57. Berlanga, M.; Montero, M. T.; Fernández-Borrell, J.; Guerrero, R., Rapid
25 spectrofluorometric screening of poly-hydroxyalkanoate-producing bacteria from microbial
26 mats. *Int. Microbiol.* 2006, 9(2), 95-102.
- 27 58. Pflüger-Grau, K.; Chavarría, M.; de Lorenzo, V., The interplay of the EIIA^{Ntr} component of
28 the nitrogen-related phosphotransferase system (PTS^{Ntr}) of *Pseudomonas putida* with
29 pyruvate dehydrogenase. *Biochim. Biophys. Acta* 2011, 1810 (10), 995-1005.
- 30 59. Hanahan, D.; Meselson, M., Plasmid screening at high colony density. *Methods Enzymol.*
31 1983, 100, 333-342.

- 1 60. Durfee, T.; Nelson, R.; Baldwin, S.; Plunkett, G.; Burland, V.; Mau, B.; Petrosino, J. F.; Qin,
2 X.; Muzny, D. M.; Ayele, M.; Gibbs, R. A.; Csörgő, B.; Pósfai, G.; Weinstock, G. M.;
3 Blattner, F. R., The complete genome sequence of *Escherichia coli* DH10B: Insights into
4 the biology of a laboratory workhorse. *J. Bacteriol.* 2008, 190(7), 2597-2606.
- 5 61. Norrander, J.; Kempe, T.; Messing, J., Construction of improved M13 vectors using
6 oligodeoxynucleotide-directed mutagenesis. *Gene* 1983, 26(1), 101-6.
- 7 62. Peoples, O. P.; Sinsky, A. J., Poly-b-hydroxybutyrate (PHB) biosynthesis in *Alcaligenes*
8 *eutrophus* H16. Identification and characterization of the PHB polymerase gene (*phbC*). *J.*
9 *Biol. Chem.* 1989, 264(26), 15298-15303.

10

11

1

TABLES

2

3 Table 1. Bacterial strains and plasmids used in this study.

4

Strain or plasmid	Description ^a	Source or reference
<i>Escherichia coli</i>		
DH5 α	Cloning host; F ⁻ λ^- <i>endA1 glnX44(AS) thiE1 recA1 relA1 spoT1 gyrA96(Nal^R) rfbC1 deoR nupG Φ80(<i>lacZ</i>ΔM15) Δ(<i>argF-lac</i>)U169 <i>hsdR17(rk- mk⁺)</i></i>	Hanahan and Meselson ⁵⁹
DH10B	Cloning host; F ⁻ λ^- <i>endA1 recA1 galK galU Δ(ara-leu)7697 araD139 deoR nupG rpsL Φ80(<i>lacZ</i>ΔM15) mcrA Δ(<i>mrr-hsdRMS-mcrBC</i>) Δ<i>lacX74</i></i>	Durfee et al. ⁶⁰
BW25113	Wild-type strain; F ⁻ λ^- Δ (<i>araD-araB</i>)567 Δ <i>lacZ4787(::rrnB-3) rph-1 Δ(rhaD-rhaB)568 hsdR514</i>	Datsenko and Wanner ⁴⁴
Plasmids		
pSEVA238	Expression vector; <i>oriV</i> (pBBR1), XylS/ <i>Pm</i> expression system; Km ^R	Silva-Rocha et al. ³⁷
pSEVA637	Cloning vector; <i>oriV</i> (pBBR1), promoter-less <i>GFP</i> ; Gm ^R	Silva-Rocha et al. ³⁷
pSEVA237R	Cloning vector; <i>oriV</i> (pBBR1), promoter-less <i>mCherry</i> ; Km ^R	Silva-Rocha et al. ³⁷
pSEVA341	Cloning vector; <i>oriV</i> (pRO1600/ColE1); Cm ^R	Silva-Rocha et al. ³⁷
pS238-Nla	Derivative of vector pSEVA238 used for regulated expression of <i>nia</i> , encoding the potyvirus Nla protease; XylS/ <i>Pm</i> \rightarrow <i>nia</i> ; Km ^R	This work
pS341T	Derivative of vector pSEVA341 carrying the constitutive P _{<i>tetA</i>} promoter; Cm ^R	This work
pS341T- <i>gfp</i>	Derivative of vector pSEVA341T used for constitutive expression of <i>gfp</i> ; P _{<i>tetA</i>} \rightarrow <i>gfp</i> ; Cm ^R	This work
pS341T- <i>gfp</i> ^{*b}	Derivative of vector pSEVA341T used for constitutive expression of a variant of <i>gfp</i> (<i>gfp</i> [*]); P _{<i>tetA</i>} \rightarrow <i>gfp</i> [*] ; Cm ^R	This work

pS341T· <i>mCherry</i>	Derivative of vector pSEVA341T used for constitutive expression of <i>mCherry</i> , $P_{tetA} \rightarrow mCherry$, Cm ^R	This work
pS341T· <i>mCherry</i> ^{*b}	Derivative of vector pSEVA341T used for constitutive expression of a variant of <i>mCherry</i> (<i>mCherry</i> [*]); $P_{tetA} \rightarrow mCherry^*$; Cm ^R	This work
pFENIX· <i>gfp</i> [*]	Derivative of plasmid pS341T· <i>gfp</i> [*] in which <i>gfp</i> has been tagged with <i>nia</i> and <i>ssrA</i> recognition targets; Cm ^R	This work
pFENIX· <i>mCherry</i> [*]	Derivative of plasmid pS341T· <i>mCherry</i> in which <i>mCherry</i> has been tagged with <i>nia</i> and <i>ssrA</i> recognition targets; Cm ^R	This work
pAeT41	Derivative of vector pUC18 ⁶¹ bearing a ca. 5-kb <i>SmallEcoRI</i> DNA fragment from <i>Cupriavidus necator</i> spanning the <i>phaC1AB1</i> gene cluster; Ap ^R	Peoples and Sinskey ⁶²
pAeT41·PHA [*]	Derivative of plasmid pAeT41 in which <i>phaA</i> has been tagged with <i>nia</i> and <i>ssrA</i> recognition targets; Ap ^R	This work
pS341·PHA	Derivative of vector pSEVA341 carrying the <i>phaC1AB1</i> gene cluster; Cm ^R	This work
pFENIX·PHA [*]	Derivative of vector pSEVA341 in which <i>phaA</i> has been tagged with <i>nia</i> and <i>ssrA</i> recognition targets; Cm ^R	This work

1

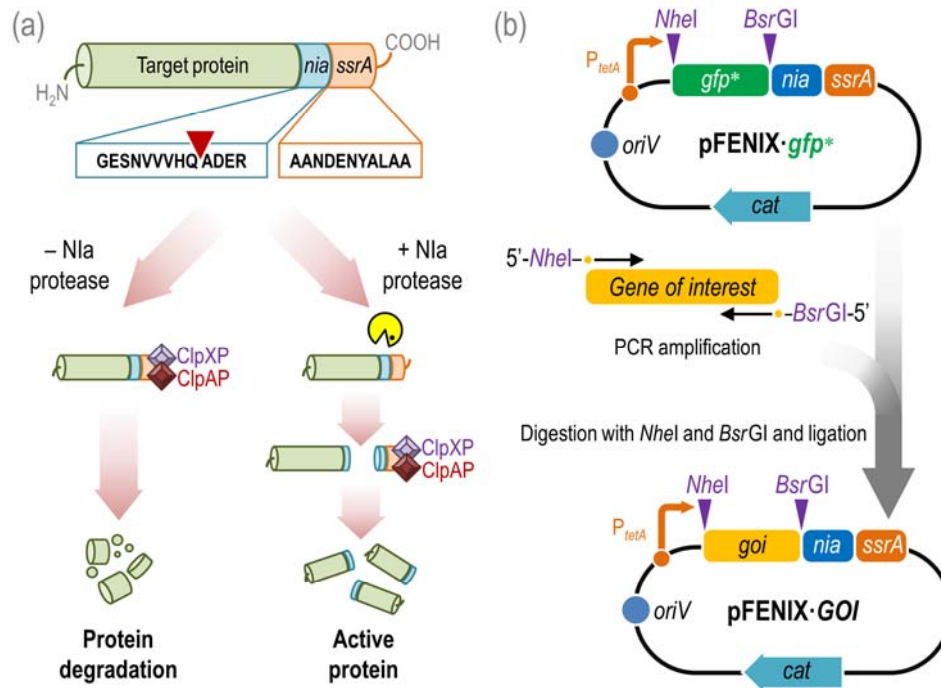
2 ^a *Antibiotic markers*: Ap, ampicillin; Cm, chloramphenicol; Gm, gentamycin; Km, kanamycin;
3 Nal, nalidixic acid.

4 ^b Modified variants of the GFP and mCherry fluorescent proteins were designed to have
5 exactly the same amino acid sequence as the proteolizable versions after the action of the
6 Nla protease.

7

FIGURES

FIG. 1. Rationale and construction of the *FENIX* system.



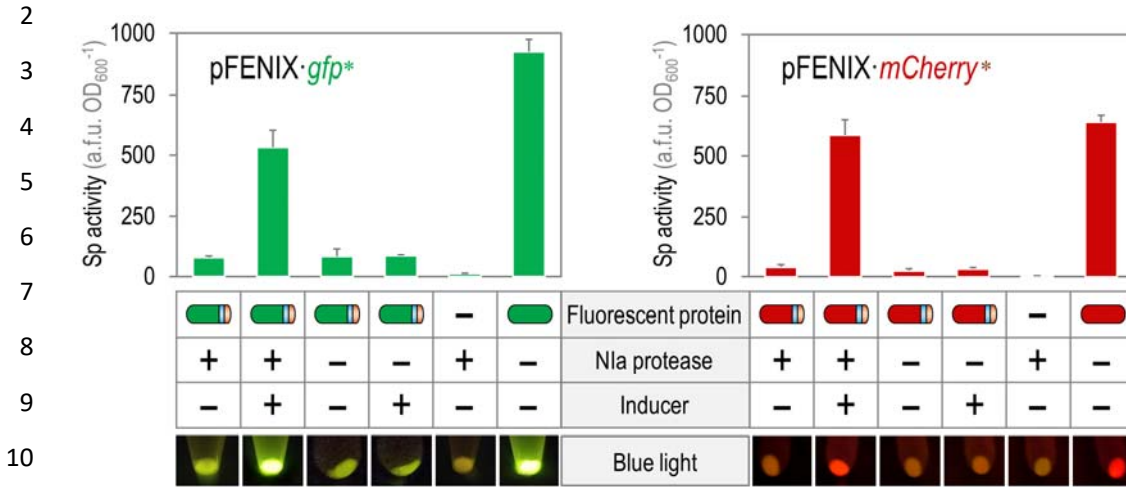
(a) Nla- and SsrA-dependent post-translational control of target proteins with the *FENIX* system.

The gene encoding the target polypeptide is added with a synthetic *nia/ssrA* tag, resulting in a hybrid protein in which the C-terminal domain displays the GESNVVHQADER·AANDENYALAA amino acid sequence. The SsrA tag is directly recognized by the ClpXP and ClpAP proteases of the bacterial proteasome *in vivo*, thus degrading the protein. Upon action of the specific potyvirus

Nla protease (the recognition site in the synthetic *nia/ssrA* tag is indicated with an inverted red triangle in the diagram), the SsrA tag is released and the polypeptide can be accumulated.

(b) *FENIX* plasmids for one-step cloning and tagging of individual target proteins. The gene encoding the target polypeptide (gene of interest, *goi*) is amplified by PCR with specific oligonucleotides that include *NheI* and *BsrGI* restriction sites. The resulting amplicon can be directly cloned into plasmid pFENIX·*gfp** (which contains a *nia/ssrA* tagged version of the green fluorescent protein) upon digestion with these two restriction enzymes. In pFENIX plasmids, the expression of the *nia/ssrA*-tagged variant of the *goi* depends on the constitutive P_{tetA} promoter.

1 FIG. 2. Evaluation of the *FENIX* system in recombinant *E. coli* using fluorescent proteins.



12 Plasmids pFENIX-*gfp** and pFENIX-*mCherry**, which contain the corresponding *nla/ssrA*-tagged

13 versions of the fluorescent proteins (schematically indicated with blue and orange strips,

14 respectively), were individually transformed into *E. coli* DH10B carrying plasmid pS238-Nla. Multi-

15 well microtiter plates containing LB medium with the necessary antibiotics and additives (using 3-

16 methylbenzoate at 1 mM as the inducer for *nla* expression, see *Methods* section), were

17 inoculated with a culture of the corresponding strain previously grown overnight in LB medium

18 with the necessary antibiotics. Cells were grown at 37°C with rotary agitation, and fluorescence

19 and bacterial growth (expressed as the optical density measured at 600 nm, OD₆₀₀) were

20 recorded after 24 h. The specific (Sp) activity of the fluorescent proteins under study was

21 calculated as the arbitrary fluorescence units (a.f.u.) normalized to the OD₆₀₀. Each bar

22 represents the mean value of the Sp activity ± standard deviation calculated from at least three

23 independent experiments. The lower panel shows bacterial pellets harvested from shaken-flask

24 cultures after 24 h of incubation under the same growth conditions indicated for the microtiter-

25 plate cultures as observed under blue light.

26

1

FIG. 3. Flow cytometry analysis of the *FENIX* system.

2

3

4

5

6

7

8

9

10

11

12

13

14

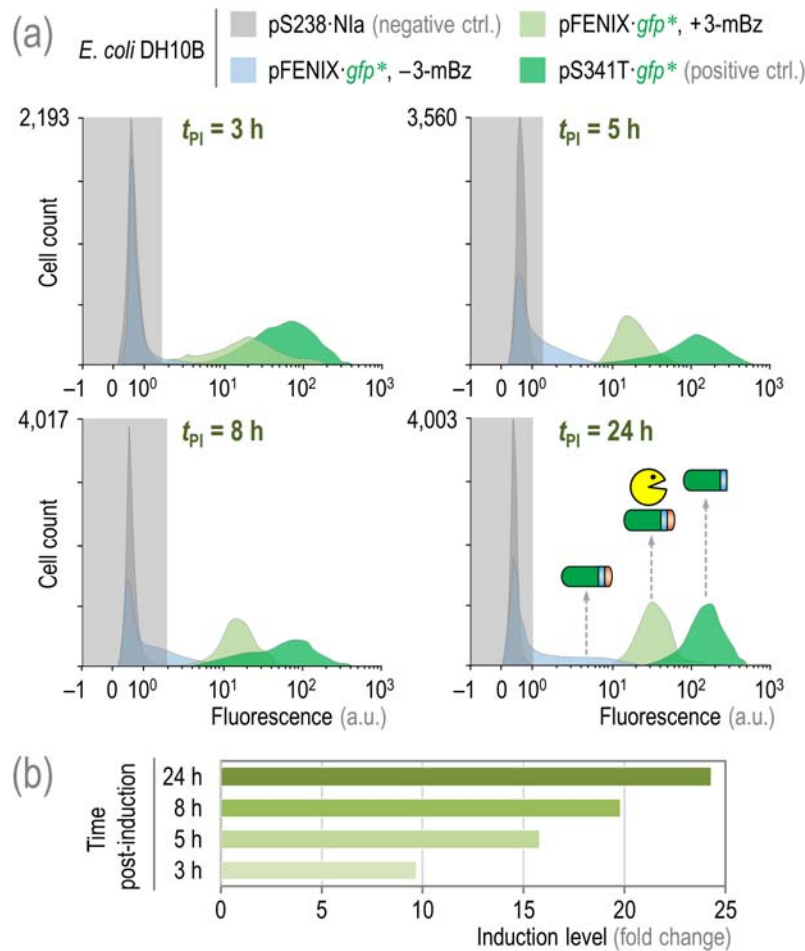
15

16

17

18

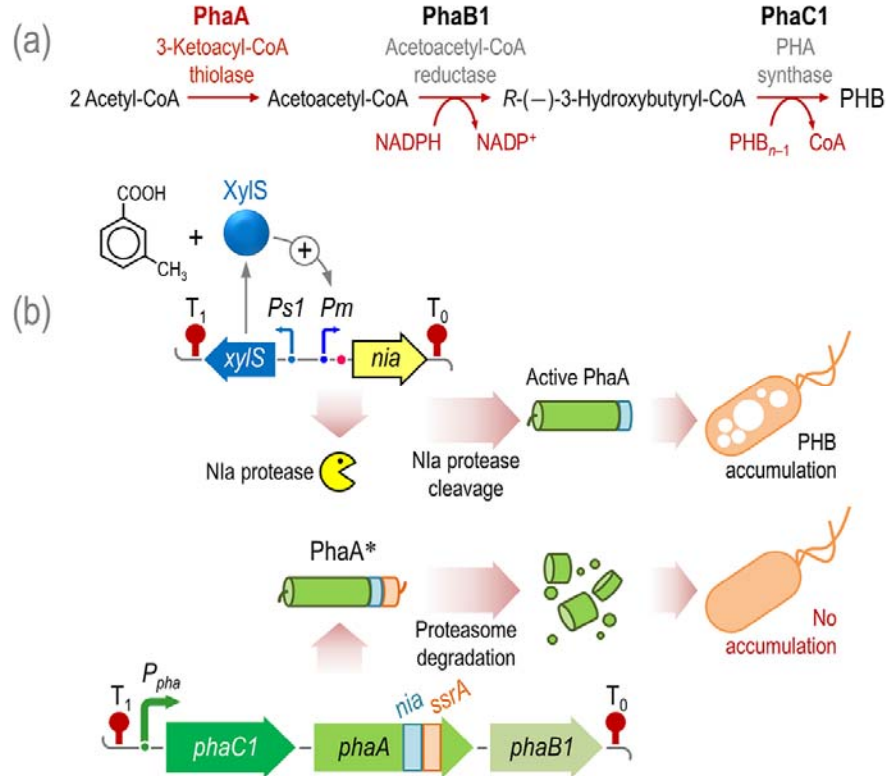
19



20 (a) Time-lapse flow cytometry analysis of GFP* fluorescence (in arbitrary units, a.u.) in shaken-
 21 flask cultures of *E. coli* DH10B carrying the plasmids indicated. Cells were grown in LB medium at
 22 37°C with rotary agitation with the appropriate antibiotics and additives explained in the *Methods*
 23 section, and samples were taken at selected times post-induction (t_{PI}). The induction of the
 24 *FENIX* system was achieved by addition of 3-methylbenzoate (3-mBz) to the cultures at 1 mM at
 25 the onset of the cultivation. The light grey rectangle in each histogram plot identifies the region
 26 considered negative for the fluorescence signal (as assessed with cells carrying plasmid
 27 pS238-Nla). The structure of the *nia/ssrA*-tagged GFP and variants thereof is schematically
 28 shown in the last panel (the blue and orange strips represent the Nla and SsrA tags, respectively)
 29 along with the Nla protease (in yellow). Note that a modified version of GFP, displaying exactly
 30 the same amino acid sequence of GFP* after proteolysis, has been used as a positive control
 31 (ctrl.). (b) Induction levels of the *FENIX* system as calculated from flow cytometry experiments.

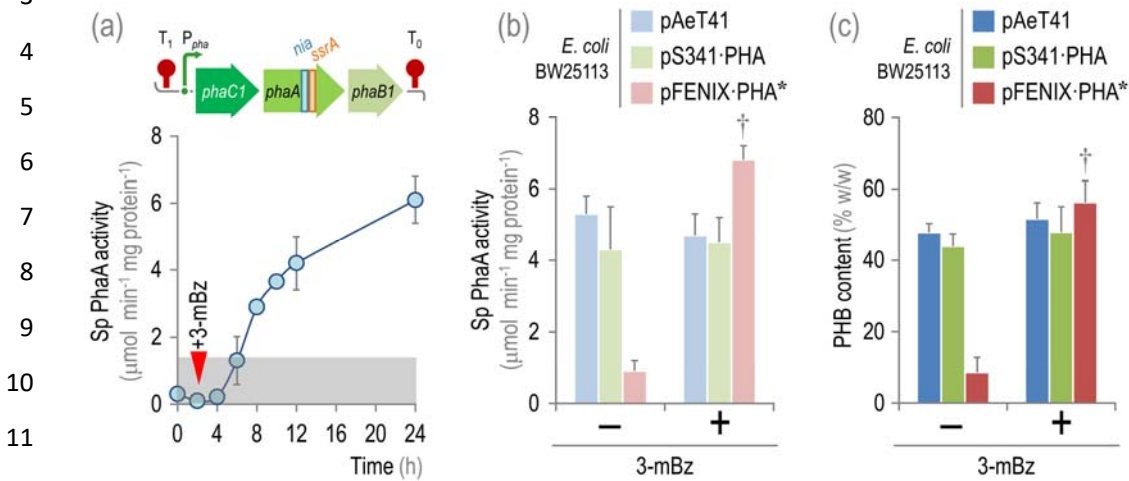
32

FIG. 4. Rationale of the *FENIX*-based metabolic switch designed for controlled biopolymer



(a) Poly(3-hydroxybutyrate) (PHB) biosynthesis pathway. Three enzymes are necessary for the *de novo* biosynthesis of PHB in *Cupriavidus necator*: 3-ketoacyl-coenzyme A (CoA) thiolase (PhaA, key step of the route as highlighted in the scheme), NADPH-dependent 3-acetoacetyl-CoA reductase (PhaB1), and PHA synthase (PhaC1). PhaA and PhaB1 catalyze the condensation of two molecules of acetyl-CoA to 3-acetoacetyl-CoA and the reduction of acetoacetyl-CoA to *R*(-)-3-hydroxybutyryl-CoA, respectively. PhaC1 polymerizes the resulting C4 monomers into PHB, whereas one CoA-SH molecule is released per monomer. PHB is stored as water-insoluble granules in the cytoplasm of the cells. (b) Synthetic circuit based on the *FENIX* system for controlled PHB accumulation. PhaA has been earmarked with the synthetic Nla/SsrA tag in the C-terminal domain (PhaA*), thus rendering the polypeptide susceptible to proteolysis by the bacterial proteasome. Under these circumstances, no PHB is accumulated by the cells. Upon activation of the Nla protease (from a separate plasmid, in which the *XylS/Pm*-dependent expression of *nia* can be triggered by addition of 3-methylbenzoate to the culture medium), the SsrA tag is removed from the protein, the active PhaA enzyme accumulates in the cells and so does PHB. The genetic elements in this scheme are not drawn to scale.

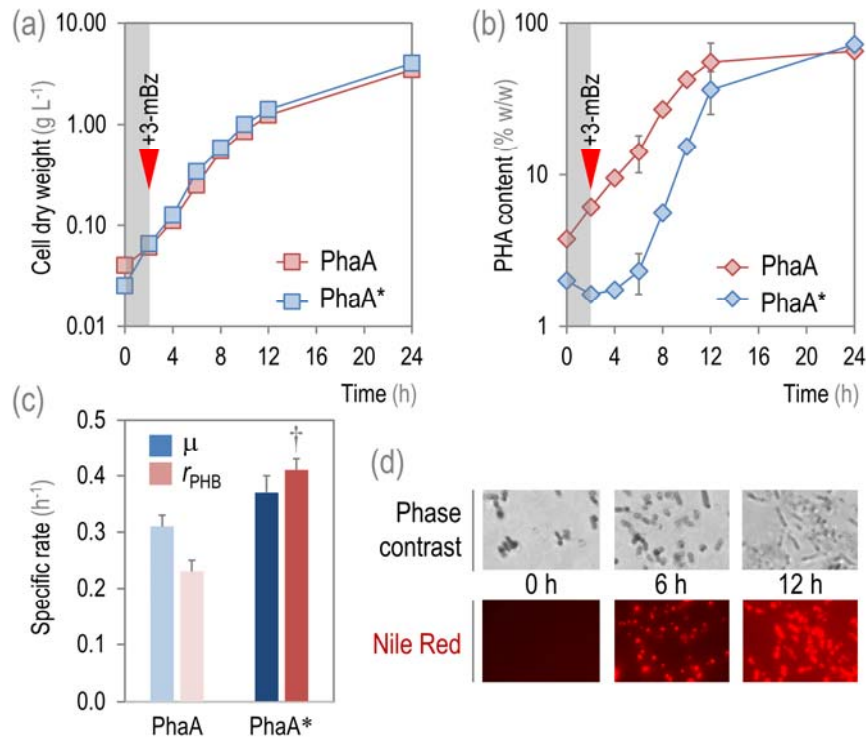
1 FIG. 5. Physiological and biochemical characterization of *E. coli* strains carrying the *FENIX*
2 system tailored for controlled PHB accumulation.



13 (a) *In vitro* determination of the specific (Sp) 3-ketoacyl-coenzyme A thiolase (PhaA) activity. *E.*
14 *coli* BW25113 was transformed both with plasmids pS238-Nla and pFENIX-PHA* (the structure of
15 the *nia/ssrA*-tagged variant of *phaA* in the *phaC1AB1* gene cluster of *C. necator* is schematically
16 shown in the upper part of the figure), and the PhaA activity was periodically determined in cell-
17 free extracts as detailed in *Methods*. The inverted red triangle indicates the addition of 3-
18 methylbenzoate (3-mBz) at 1 mM to the culture medium; the gray bar identifies the maximum
19 thiolase activity detected in *E. coli* BW25113 transformed only with plasmid pS238-Nla. (b) *In*
20 *vitro* determination of the Sp PhaA activity and (c) PHB accumulation in *E. coli* BW25113 carrying
21 vector pS238-Nla and the indicated plasmids. Plasmids pAeT41 and pS341-PHA express the
22 native *phaC1AB1* gene cluster of *C. necator* in different vector backbones. In all plasmids used in
23 these experiments, the expression of the *pha* gene cluster is driven by the native, constitutive
24 P_{pha} promoter. All shaken-flask cultures shown in this figure were carried out in LB medium added
25 with 30 g L⁻¹ glucose and the adequate antibiotics and additives specified in *Methods*. Each
26 parameter is reported as the mean value ± standard deviation from duplicate measurements in at
27 least three independent experiments. Significant differences ($P < 0.05$, as evaluated by means of
28 the Student's *t* test) in the pair-wise comparison of induced *versus* non-induced cultures are
29 indicated by the † symbol.

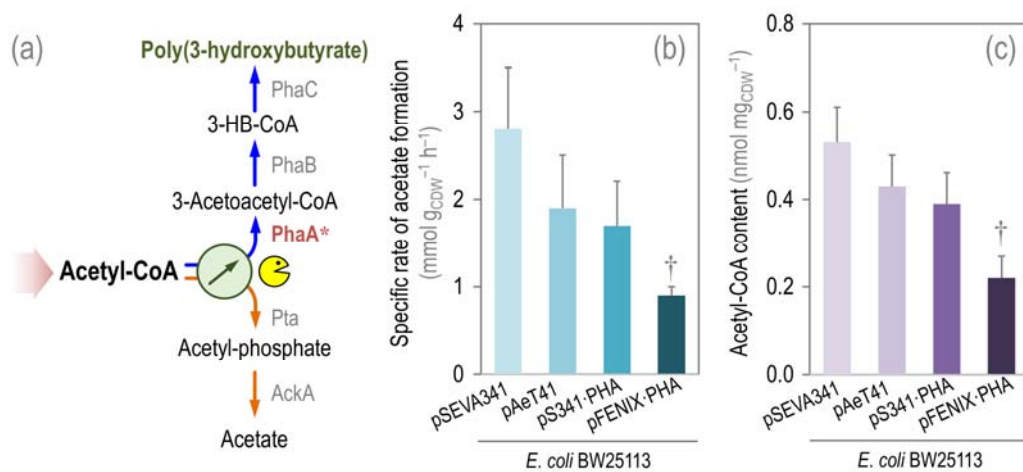
30

FIG. 6. Growth and PHB accumulation by recombinant *E. coli* carrying PhaA*.



(a) Bacterial growth, expressed as the density of cell dry weight, and (b) PHB content on biomass in shaken-flask cultures of *E. coli* BW25113/pS238-N1a transformed either with plasmid pS341-PHA (expressing the native *pha* gene cluster, identified as PhaA) or pFENIX-PHA* (expressing the *nia/ssrA*-tagged variant of *phaA*, identified as PhaA*). The inverted red triangle indicates the addition of 3-methylbenzoate (3-mBz) at 1 mM to the culture medium (M9 minimal medium containing 30 g L⁻¹ glucose); the gray bar also identifies the time pre-induction of the system. (c) Specific rates of bacterial growth (μ) and PHB accumulation (r_{PHB}) in the strains under study. Significant differences ($P < 0.05$, as evaluated by means of the Student's *t* test) in the pairwise comparison between the two strains is indicated by the † symbol. In the graphics (a-c), each parameter is reported as the mean value \pm standard deviation from duplicate measurements in at least three independent experiments. (d) Qualitative assessment of PHB accumulation in samples taken from shaken-flask cultures at the indicated times and stained with the lipophilic Nile Red dye. Stained cells were observed under the microscope either under phase contrast or fluorescence as indicated in *Methods*.

1 FIG. 7. Establishing an orthogonal metabolic switch at the acetyl-CoA node based on the
2 *FENIX* system.



3
4
5
6
7
8
9
10
11
12 (a) The acetyl-coenzyme A (CoA) metabolic node in the *E. coli* recombinants used in this study.
13 The wide shaded arrow represents the central pathways leading to acetyl-CoA formation (i.e.
14 glycolysis); this intermediate is used as a precursor in a myriad of metabolic reactions (not
15 indicated in the scheme). The main sinks of acetyl-CoA are shown, namely, PHB biosynthesis or
16 acetate formation (catalyzed by Pta, phosphotransacetylase, and AckA, acetate kinase). The Nla
17 protease of the *FENIX* system, mediating the metabolic switch, is indicated in yellow. (b) Specific
18 rate of acetate formation, as determined by secretion of acetate into the culture medium. (c)
19 Intracellular content of acetyl-CoA, evaluated by LC-MS in cell extracts as explained in *Methods*.
20 All shaken-flask cultures shown in this figure were carried out in M9 minimal medium added with
21 30 g L⁻¹ glucose and the adequate antibiotics and additives specified in *Methods*. *E. coli*
22 BW25113 was transformed with plasmid pS238-Nla in all cases. Each parameter is reported as
23 the mean value ± standard deviation from duplicate measurements in at least two independent
24 experiments. Significant differences ($P < 0.05$, as evaluated by means of the Student's *t* test) in
25 the pair-wise comparison of each recombinant against the control strain (carrying the empty
26 pSEVA341 vector) are indicated by the † symbol. *3-HB-CoA*, *R*(-)-3-hydroxybutyryl-CoA; *CDW*,
27 cell dry weight.